Vortex generation induced by low-frequency wire vibration in superfluid ^{3}He-*B*

Y. Nago,* M. Inui, R. Kado, K. Obara, H. Yano, O. Ishikawa, and T. Hata
Graduate School of Science, Osaka City University, Osaka 558-8585, Japan
(Received 20 October 2010; published 14 December 2010)

We report the generation of a quantized vortex in superfluid ^{3}He-B. Oscillating objects can generate vortices due to breaking of Cooper pairs in superfluid ^{3}He, resulting that the threshold velocity for vortex generation is higher than the pair-breaking velocity. Using very-low-frequency vibrating wires with smooth surfaces, however, we find that the threshold velocity of vortex generation is lower than the pair-breaking velocity. The threshold velocity remains constant with decreasing ^{3}He pressure until the pair-breaking velocity equals the vortex-generation threshold velocity at a low pressure. These results indicate that another mechanism that is independent of pressure generates vortices for the low-frequency vibrating wire in superfluid ^{3}He. The threshold velocity observed in experiments turns out to be nearly equal to the velocity of the instability of the vortex lines attached to the wire, which is characterized by only the circulation quantum.

DOI: 10.1103/PhysRevB.82.224511 PACS number(s): 67.25.dk, 67.30.he, 47.15.Cb, 47.27.Cn

I. INTRODUCTION

Quantized vortices and quantum turbulence in superfluid helium have been extensively studied for a long time.[1] A quantized vortex is a stable topological defect with quantized circulation; quantum turbulence is simply a tangle of quantized vortices. Consequently, turbulence generation mechanisms in superfluid helium are expected to be much simpler than those in classical fluids. There are two main kinds of turbulence generation processes in an inviscid superfluid: intrinsic and extrinsic processes. In intrinsic processes, many vortices are thought to nucleate at a flow velocity around the Landau critical velocity at which superfluidity breaks down. Intrinsic vortex nucleation has been observed in superfluid ^{4}He in various experiments including ion experiments[2] and flow experiments through an aperture.[3] Such experiments have revealed that vortices nucleate at a flow velocity on the order of 1–10 m/s, which is slightly lower than the Landau critical velocity of 60 m/s.[4] In contrast, remanent vortices play an important role in generating turbulence in extrinsic processes. Vortices that are spontaneously nucleated during cooling through the superfluid transition[5] remain firmly attached to heterogeneous boundaries.[6] Attached vortices expand unstably and create many vortices by superflow. Turbulence generation due to remanent vortices has been observed by vibrating an object, such as spheres,[7] wires,[8] grids,[9] and quartz tuning forks.[10] Experiments have revealed that turbulence is generated at an oscillating velocity of around 50 mm/s even at the zero-temperature limit, which is much smaller than the Landau critical velocity. In addition, vibrating-wire measurements[11] recently revealed that remanent vortices that form bridges between the wire and surrounding boundaries generate turbulence. Numerical simulations[12] have shown that in oscillatory flow Kelvin waves are generated on bridge vortex lines that are attached to an oscillating object and a wall. These vortex lines become unstable and create vortex rings and turbulence at sufficiently high flow velocities.

Generation of turbulence in superfluid ^{3}He-B has also been studied using oscillating objects.[13,14] Unlike for superfluid ^{4}He, the turbulence generation mechanism observed in oscillating superfluid ^{3}He-B is intrinsic: vortices are generated by pair breaking.[10,13] Since the Landau critical velocity in superfluid ^{3}He is three orders of magnitude lower than that in superfluid ^{4}He, object oscillation can easily break Cooper pairs at a low velocity. Vibrating-wire measurements[15] revealed that when $T/T_c < 0.2$, where T_c is the transition temperature of the superfluid, Cooper pairs break at an oscillating velocity of about 9 mm/s at 0 bar and turbulence is generated exceeding that velocity. Vortex seeds appear to be generated by pair breaking, growing into a tangle of vortices by the oscillation of the object.

As was the case for superfluid ^{4}He, remanent vortices are expected to remain attached to heterogeneous boundaries in superfluid ^{3}He (Ref. 16) and oscillatory flow can cause the Kelvin waves on the remanent vortex lines attached to the object to become unstable.[12] Therefore, remanent vortices are expected to cause turbulence in superfluid ^{3}He-B if they are attached to an oscillator. However, the very-low-pair-breaking velocity makes it difficult to observe this turbulence generation. Furthermore, the surface roughness of the oscillating object is closely related to the threshold velocity of pair breaking and intrinsic vortex generation:[17] an oscillating object with rough surfaces locally enhances ambient superfluid flow, which can cause pair breaking at velocities below 9 mm/s.[18] In a vibrating-grid measurement,[14] Lancaster group observed damping due to vortex generation at a velocity of about 1 mm/s and discussed the instability of the Kelvin waves on vortices attached to the grid mesh. However, a recent theoretical study[12] suggests that a contribution from pair breaking cannot be ruled out since the grid has much rougher surfaces than a vibrating wire and the mesh has some sharp edges, which should strongly enhance flow. This illustrates the difficultly of studying the turbulent transition. Oscillating objects with smooth surfaces are preferable for observing turbulence due to remanent vortices.

An oscillating object can generate a Kelvin wave on bridge vortex lines attached to the object and a surrounding boundary. An oscillation with an amplitude greater than the wavelength of the Kelvin wave may cause the wave to be unstable, resulting in turbulence being generated.[19] The dispersion relation for a Kelvin wave is given by

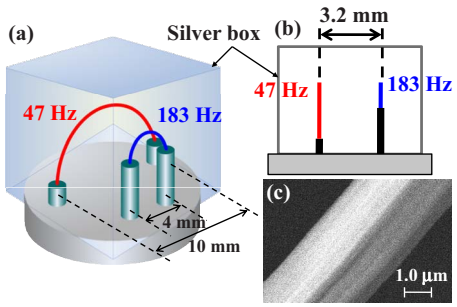

FIG. 1. (Color online) Configuration of vibrating wires with resonance frequencies of 47 and 183 Hz: (a) overview and (b) side view. (c) Electron micrograph of the surface of the 47 Hz vibrating wire. The two vibrating wires have almost the same surface roughnesses. The distance between the legs of the two wire loops are 10 mm for the 47 Hz wire and 4 mm for the 183 Hz wire. The two wires are parallel to each other and are separated by a distance of 3.2 mm. A silver box is used to cover the assembly.

$$\omega \approx \frac{\kappa k^2}{4\pi} \ln\left(\frac{1}{k a_0}\right). \tag{1}$$

Here κ is the circulation quantum, a_0 is a radius of the vortex core, which is corresponding to the superfluid coherence length, and k is $2\pi/\lambda$, where λ is the wavelength. Since the oscillation amplitude is given by v/ω, the velocity at which the wave becomes unstable is nearly proportional to $\sqrt{\omega}$, which can be derived from Eq. (1). In a previous study,[20] we found that a vibrating wire with a resonance at 183 Hz can generate vortices at velocities above the pair-breaking velocity. However, a vibrating wire with a resonance frequency of 47 Hz can generate vortices below the pair-breaking velocity. In the present study, we investigate the onset of vortex generation using vibrating wires with two different resonances frequencies (47 and 183 Hz) as a function of ^{3}He pressure. We discuss the vortex-generation mechanism.

II. EXPERIMENTAL

Figure 1 shows the experimental setup. The two vibrating wires are fabricated from identical multifilaments, made of 3 μm NbTi filaments. We know from a previous experiment[21] that a bundle of multifilaments contains filaments with different roughnesses. In the present study, we selected smoother filaments with a roughness of $\sim$100 nm for the two vibrating wires [see Fig. 1(c)] in an attempt to prevent local flow in the vicinity of the wire from causing local pair breaking at low wire velocities. The distances between the legs of the two wire loops are 10 mm and 4 mm, respectively. The two wires are parallel to each other and are separated by a distance of 3.2 mm. The assembly is covered with a silver box. We placed the wires and the silver box in the cell used in a previous study.[22] The temperature was measured using a Pt-NMR thermometer located near the wires in the cell so as to obtain the temperature of the bulk liquid directly. The cell was mounted on a copper nuclear stage and cooled to temperatures of $0.17T_c$–$0.25T_c$ by adiabatic demagnetization.

The vibrating wires were driven by ac electric currents in a magnetic field of 27.4 mT, resulting in resonance frequencies in vacuum of 47 Hz for the wire in a 10 mm loop and 183 Hz for the wire in a 4 mm loop. Q value is 1490 for the 47 Hz wire and 1740 for the 183 Hz wire in vacuum. We simultaneously measured a Faraday voltage V_{rms} induced by wire oscillation in a field B=27.4 mT and its resonance frequency using a phase-locked loop technique.[8] A peak velocity of the apex of the wires is calculated by $v=\sqrt{2}V_{rms}/cBl$, where l is the distance between the legs of the wire loop and c is a geometrical constant. We assume the wire loop to be semicircular shape, which gives $c=\pi/4$. We filled the cell with ^{3}He liquid up to the filling line and adjusted the liquid pressure to 1, 10, 20, and 28 bars to investigate the relation between pair breaking and vortex generation over a range of pressures. Experiments were performed using the two wires: the 183 Hz wire was used as a vortex generator and the 47 Hz wire was used as a vortex detector, and vice versa. We applied a low driving force to the detector and simultaneously measured the generator and detector responses while increasing the driving force of the generator.

III. RESULTS AND DISCUSSION

A. Responses of vibrating wires in superfluid ^{3}He-B

The velocity responses of a vibrating wire as a function of driving force exhibit well-known characteristics, which have been observed in previous studies.[15,20] The lower panels of Figs. 2 and 3 show the responses of the 183 and 47 Hz vibrating wires as a function of driving force at each of the four pressures, respectively. Both vibrating wires exhibit similar behavior. The nonlinear increase in the velocity at low driving forces is caused by the strongly modified excitation spectrum due to superflow and Andreev reflection of quasiparticle excitations.[23] The additional suppression of the velocity at high driving forces is caused by damping due to pair breaking. The threshold velocity for pair breaking is almost the same for both vibrating wires. It increases with increasing pressure, as indicated by the arrows in Figs. 2 and 3. Also, the measurements at different temperatures reveal that this velocity is almost constant as a function of temperature up to about $0.25T_c$ at all four pressures. The measurements results for a single vibrating wire at low pressures have been reported previously.[15,24] They reveal that the onset of pair breaking depends on pressure and temperature, which is consistent with the present results. We extended the pressure range up to 28 bars in this study and found that the F-v characteristics are consistent at all pressures in this range, independent of frequency.

We also measured the velocity responses of the detector at a low constant driving force simultaneously with the generator profiles to detect quasiparticle excitation propagating from the generator. The upper panels in Fig. 2 show the responses of the 47 Hz detector as a function of the driving force of the 183 Hz generator. The profile of the detector response reveals that the detector velocity generally tends to decrease with increasing generator driving force despite a constant driving force being applied to the detector. At low temperatures such as $\sim 0.2T_c$, thermal damping of wire os-

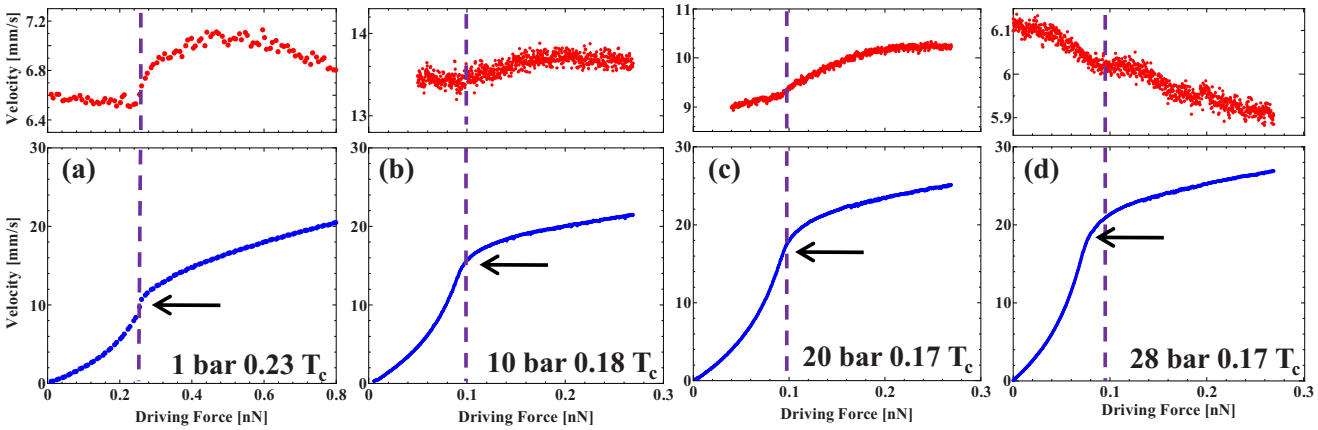

FIG. 2. (Color online) Responses of a vibrating wire with a resonance at 183 Hz measured at (a) 1 bar, (b) 10 bars, (c) 20 bars, and (d) 28 bars, as a function of driving force (lower panels). The arrows indicate the pair-breaking threshold velocities. The upper panels show plots of the responses of a 47 Hz vibrating wire with a fixed driving force, which were measured simultaneously with the responses of the 183 Hz vibrating wire. The broken lines indicate the driving forces at which a reduction in damping is observed in the response of the 47 Hz vibrating wire, indicating vortex generation by the 183 Hz vibrating wire.

cillation at low velocities is dominated by ballistic quasiparticle excitations of ^{3}He. This indicates that generator oscillation increases thermal excitations, which increases the damping of detector oscillation. However, the detector velocity increases with a kink near the onset of pair breaking in the generator velocity, as indicated by the point at which the broken line intersects each velocity curve in Fig. 2. This indicates a reduction in damping of detector oscillation due to vortices screening thermal excitations.[13,20] When vortices are generated by vibrations of the generator, they propagate to the detector. The thermal excitations then undergo Andreev reflection by vortices around the detector, which reduces damping of detector oscillation, i.e., increases the detector velocity. In the present experiments, we operated the detector at somewhat high velocities to improve signal-to-noise ratios, though low-velocity oscillation would be better to avoid the Andreev effect and additional heating. The detector velocity appears to increase until the vortex density saturates around the wire, after which damping of detector oscillation by thermal excitations becomes dominant, reducing the detector velocity again, as shown in Fig. 2.

The 183 Hz detector exhibits a similar behavior to the 47 Hz detector, as shown in the upper panels in Fig. 3. Vortex generation by the generator can be identified from the increase in the detector velocity, which occurs at the point where the broken line intersects the velocity curve of the detector in Fig. 3. The velocity shifts due to the screening effect tend to be larger for the 183 Hz detector than those for the 47 Hz detector. This may be because the 47 Hz wire is larger in size than the 183 Hz wire as shown in Fig. 1. The 47 Hz generator has a larger active region due to a large leg spacing; thus, many vortices will be emitted with a wide spatial extent,[25] causing the strong screening effect. Unlike the case for the 183 Hz generator and 47 Hz detector, the detector velocity starts to increase before the increase in the generator velocity is suppressed, except for the case of 1 bar.

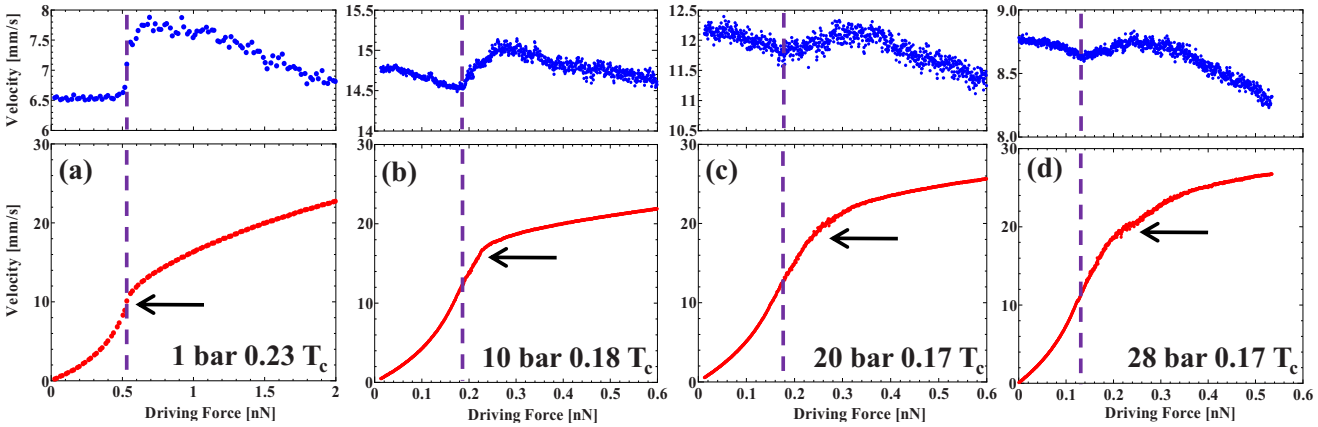

FIG. 3. (Color online) Responses of a vibrating wire with a resonance at 47 Hz measured at (a) 1 bar, (b) 10 bars, (c) 20 bars, and (d) 28 bars, as a function of driving force (lower panels). The responses of a 183 Hz vibrating wire with a fixed driving force measured simultaneously with the responses of the 47 Hz vibrating wire (upper panels). The arrows and the broken lines are explained in the caption for Fig. 2. The data for 1 bar (a) shows similar behavior as (a) in Fig. 2 whereas (b), (c), and (d) show a reduction in the damping of detector oscillation at a generator velocity lower than the pair-breaking velocity.

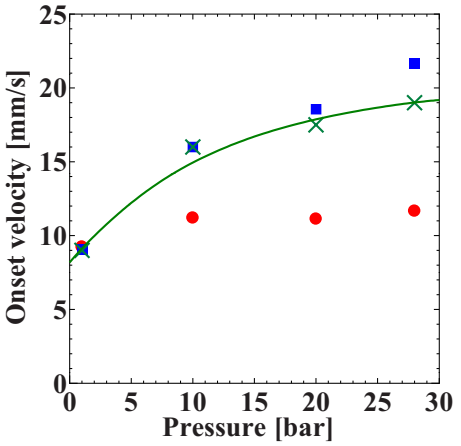

FIG. 4. (Color online) Pressure dependence of threshold velocity: circles represent vortex generation for the 47 Hz vibrating wire, squares show vortex generation for the 183 Hz vibrating wire, and the crosses indicate pair breaking. The line represents pair-breaking velocity v_p estimated from $v_p = v_L/3$, where v_L is the Landau velocity.

B. Threshold velocities for pair breaking and vortex generation

The threshold velocity for vortex generation is given by the velocity at which the broken line intersects the velocity curve of the generator in Figs. 2 and 3. Figure 4 shows a plot of the threshold velocity for vortex generation for each vibrating wire and the pair-breaking velocity (an average value roughly estimated from the responses of the 183 Hz vibrating wire) against pressure. It shows some remarkable characteristics. First, as mentioned in the previous section, the pair-breaking velocity v_p exhibits pressure dependence. It is almost constant between the 47 Hz and 183 Hz vibrating wires. This is because the pair-breaking velocity v_p is attributed to the Landau critical velocity v_L, which is independent of frequency. At the zero-temperature limit, $v_L \sim \Delta(0)/p_F$ in superfluid ^{3}He-B, where $\Delta(0)$ is the B-phase energy gap and p_F is the Fermi momentum. The pair-breaking velocity is estimated to be

$$v_p = v_L/3 = \Delta(0)/3p_F, \tag{2}$$

at all pressures, as shown in Fig. 4. A previous study[13] using a vibrating wire constructed from NbTi multifilaments reported that the pair-breaking velocity is described by Eq. (2) at 0 and 5 bars, which is consistent with our results. We found that Eq. (2) can describe the pair-breaking velocity at pressures up to 28 bar. The pair-breaking velocity is considered to be reduced by potential flow in the vicinity of a wire and by suppression of the gap due to the surface roughness of the wire on a scale of the Fermi wavelength.[24] Thus, a cylindrical wire made from the same material (NbTi) can reduce the pair-breaking velocity by a factor of 3.

Second, we found that there are two threshold velocities for vortex generation. One is the threshold velocity for the 183 Hz vibrating wire at all pressures and the 47 Hz vibrating wire at 1 bar, which is equal to or slightly higher than pair-breaking velocity v_p. The other is the threshold velocity for the 47 Hz vibrating wire at pressures of 10, 20, and 28 bars, which is lower than the pair-breaking velocity v_p (see Fig. 4).

C. Vortex generation caused by pair breaking

The results observed for the 183 Hz vibrating wire at all pressures and the 47 Hz vibrating wire at 1 bar indicate that vortex generation is caused by pair breaking. Similarly, vortex generation caused by pair breaking has been observed at a velocity slightly higher than the pair-breaking velocity in a previous vibrating-wire measurement at 0 and 5 bars.[13] In the present study performed at pressures up to 28 bars, the threshold velocity for vortex generation tends to be higher than the pair-breaking velocity at high pressures. Intrinsic vortex nucleation is not allowed without superflow with a sufficiently high energy to overcome the nucleation barrier.[17] In the case of a vibrating wire, a sufficiently high vibration velocity is required to overcome the nucleation barrier for a vortex half-ring on the wire surface. The energy of a vortex ring with radius R is given by $E = (\rho_s \kappa^2 R/2)\ln(8R/a_0)$,[4] where ρ_s is the superfluid density. The energy of a vortex half-ring with radius of $R \sim a_0$ is a minimum for $\sim \rho_s \kappa^2 a_0$. Therefore, when the kinetic energy of the superflow generated by its vibration within a volume of $\sim a_0^3$ in the vicinity of the wire exceeds the energy of the minimum vortex ring, superflow can become unstable and nucleate a vortex.[17] Hence, the critical velocity of superflow instability is estimated to be $v_{cb} \sim \kappa/a_0$. Although it is not possible to perform a quantitative evaluation based on this rough estimate (a more precise estimation is given in Ref. 17), the intrinsic limiting velocity depends on pressure and is somewhat higher than (but close to) the Landau critical velocity. This means that, although vortices can be nucleated above the Cooper-pair-breaking velocity, intrinsic vortex nucleation does not necessarily immediately follow breaking of Cooper pairs. Therefore, it is not surprising that vortices are generated at a velocity higher than the pair-breaking threshold velocity. However, this explanation does not explain why the gap between the two threshold velocities increases at higher pressures. Figure 2 shows that the onset of additional suppression due to pair breaking is not sharp at high pressures, indicating that quasiparticle excitation gradually nucleates and gives rise to energy dissipation in wire motion. This may cause the large gap between the two threshold velocities at high pressures. For a deeper discussion, further theoretical investigations into the pair-breaking and vortex-generation mechanisms are needed.

D. Vortex generation below the pair-breaking velocity

The results observed for the 47 Hz vibrating wire at 10, 20, and 28 bars reveal no relation between the pair-breaking and vortex-generation thresholds, suggesting that another vortex-generation mechanism is operative. We discuss possible vortex-generation mechanisms for the 47 Hz wire in this section.

One possible mechanism is that vortex generation is caused by pair breaking in local flow enhanced by protuberances from the wire surface. This has been observed in mea-

surements by the Lancaster group.[18] They observed pair breaking and intrinsic vortex generation at a low velocity of ~5 mm/s because their vibrating wires have rough surfaces on the scale of microns, which locally enhance ambient superfluid flow causing Cooper pairs to break easily. It has also been reported that a vibrating grid generates turbulence at ~1 mm/s;[14] the possibility of pair-breaking contribution[12] has been advanced to explain this result since the vibrating grid is much rougher than a vibrating wire. However, our vibrating wires are smoother than the vibrating wires used by the Lancaster group and grids, as shown in Fig. 1(c). Hence, the surface roughness does not seem to be sufficiently high to give rise to the enhanced local flow required to break Cooper pairs. Furthermore, the Lancaster group observed some plateaus due to vortex nucleation in the velocity responses of a vibrating wire as a function of driving force. In our case, there are no plateaus at the threshold velocity for vortex generation in Fig. 3. In Fig. 3(d), there seems to be plateau at 20 mm/s, which is higher than the vortex-generation threshold velocity, close to a pair-breaking threshold velocity. Consequently the observed vortex generation implies that a different generation mechanism is operating from that observed in previous studies.[18]

If vortices are generated for the 47 Hz vibrating wire due to pair breaking, the threshold velocity for vortex generation should depend on pressure because pair breaking is greatly influenced by the B-phase energy gap, as Eq. (2) shows. In fact, the threshold velocity for vortex generation for the 183 Hz vibrating wire shows a pressure dependence (see Fig. 4). The vortex-generation threshold for a vibrating grid has been reported to exhibit a small pressure dependence,[14] although its mechanism is uncertain. However, we find that the threshold velocity for the 47 Hz wire at 10, 20, and 28 bars is 11 mm/s, independent of pressure (see Fig. 4), indicating that the vortex-generation mechanism differs from that for pair breaking.

Since the threshold velocity of vortex generation is independent of pressure, its mechanism may be related to the motion of remanent vortex lines, which is characterized by the circulation quantum rather than the coherence length and the energy gap of ^{3}He-B. In superfluid helium, vortices are spontaneously nucleating during cooling through the superfluid transition.[5] In superfluid ^{3}He, it is also known that cosmic rays interact with helium during passing through the cell, overheating it locally above T_c and creating vortices due to subsequent fast cooling.[26] Those vortices may remain firmly if attaching to heterogeneous boundaries.[16] It is therefore plausible that vortex lines remain attached to a wire so that vortices are generated as the wire oscillates; this has been observed in previous studies that investigated vibrating wires in superfluid ^{4}He.[8,11,28] We compare our results in ^{3}He-B with those for ^{4}He to clarify the vortex-generation mechanism for the 47 Hz vibrating wire. In superfluid ^{4}He, the resonance frequency of a vibrating wire increases by about 1 Hz at the turbulent transition due to remanent vortices.[28] Figure 5 shows the responses of the resonance frequency of the 47 and 183 Hz vibrating wires in superfluid ^{3}He-B at 20 bars. The frequency f is normalized by the frequency f_1 at a velocity of 5 mm/s.[27] For both vibrating wires, the resonance frequency increases with increasing velocity

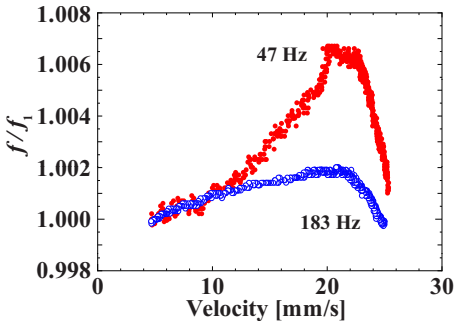

FIG. 5. (Color online) Normalized resonance frequencies f/f_1 of 47 Hz vibrating wire (●) and 183 Hz vibrating wire (○) measured at 20 bars, as a function of velocity. f_1 indicates the frequency at a velocity of 5 mm/s. The temperature for each vibrating wire is $0.17T_c$.

and abruptly decreases at high velocities exceeding the pair-breaking velocity. It is found that the velocity at which the frequency starts to decrease is equal to each other and shows the same pressure dependence as the threshold velocity for pair breaking. A stationary motion of a vibrating wire can be described by an equation of forced harmonic oscillation; the resonance frequency of a vibrating wire depends on the effective mass and the effective spring constant of the vibrating wire. The effective mass is hydrodynamically enhanced by the backflow around the wire because of its motion. When the wire moves at a sufficiently high velocity, the effect of Andreev reflection modifies the effective mass. Furthermore, presence of vortices attached to the wire surfaces is likely to affect both the effective mass and the effective spring constant. The decrease in the frequency at high velocities in Fig. 5 implies that breaking of Cooper pairs by high-velocity oscillation of the wire causes normal fluid component locally in the vicinity of the wire surfaces, resulting that the hydrodynamic mass increases. On the other hand, the mechanism of increase in the frequency at low velocities has not been clear. However, one can note that, for the 47 Hz vibrating wire in Fig. 5, the frequency seems to excessively increase exceeding the threshold velocity 11 mm/s of vortex generation. This feature was also observed for the 47 Hz vibrating wire at 10 and 28 bars. The increase in the frequency at onset of vortex generation is similar to the behavior observed for ^{4}He.[8,28] It may be possible that the 47 Hz vibrating wire generates turbulence due to remanent vortices. However, there is a remarkable difference between ^{4}He and ^{3}He-B cases that hysteresis at the onset of vortex generation for up and down sweeps of the driving force has not been observed in superfluid ^{3}He-B while observed in superfluid ^{4}He.[28] Further experimental and theoretical investigations are required to clarify the mechanism of frequency shift at the turbulent transition and the discrepancies between ^{4}He and ^{3}He-B.

Remanent vortices are considered to remain attached to heterogeneous boundaries in superfluid ^{3}He.[16] The vibrating wires used in the present study have surface roughnesses of about 100 nm [see Fig. 1(c)], comparable to the core size of a vortex in ^{3}He-B. The roughnesses may also enhance a local flow, though we did not observe pair breaking caused by an enhanced flow, as mentioned above. Vortices pinned to a

3-μm-diameter vibrating wire are considered to be submicron in size and thus wire vibration initially induces homogeneous superflow through the pinned vortices. It is considered that oscillatory flow with frequency ω can stretch vortices and cause avalanchelike multiplication of vortices into turbulence at a threshold velocity of[19]

$$v_c = \sqrt{8\kappa\omega/\beta}, \tag{3}$$

where β is a constant determined by the mutual friction coefficients. Since β is unity at temperatures as low as $\sim 0.2T_c$ due to the absence of a normal component, the turbulence threshold velocity will principally depend on the frequency and not on the shape or size of the oscillator. Thus, it is plausible that in our measurements of a low-frequency (47 Hz) vibrating wire in superfluid ^{3}He-B we observed instability in the remanent vortices attached to the wire at a velocity of ~ 11 mm/s, which is below the threshold velocity for pair breaking. Indeed, from Eq. (3), the threshold velocity for turbulence is estimated to be 12.5 mm/s at a frequency of 47 Hz, which agrees with the threshold velocity observed for the 47 Hz vibrating wire [although Eq. (3) is qualitative only]. Furthermore, this threshold velocity is independent of the pressure, as seen in Fig. 4, which is consistent with Eq. (3). Thus, we cannot observe vortex generation at 1 bar because vortices are generated by pair breaking at velocities below 9 mm/s before the remanent vortices become unstable. On the other hand, for a velocity of 11 mm/s at a frequency of 47 Hz, Eq. (3) predicts that the threshold velocity for turbulence will be 21.7 mm/s at a frequency of 183 Hz. However, Cooper pairs break and many vortices are generated below 20 mm/s. This may be why vortex generation due to remanent vortices cannot be observed for the 183 Hz vibrating wire.

Another process of the instability of vortex lines attached to a boundary by an oscillatory superfluid flow has been recently studied by numerical simulations.[12] These simulations predict that Kelvin waves with a frequency corresponding to the oscillation frequency are generated on vortex lines attached to a stationary sphere and that these waves expand and create many vortex rings at high flow velocities. A similar behavior is expected to occur for a vibrating wire because the oscillatory motion of a wire can generate Kelvin waves on vortex lines attached to it. We assume that vortices attached to the 47 Hz wire cause the instability of the Kelvin wave at a wire velocity of 11 mm/s. Wire vibration with a frequency ω can induce the Kelvin wave with a wave number k according to Eq. (1), and the Kelvin waves may become unstable when the oscillation amplitude $A=2v/\omega$ is approximately equal to the wavelength of the Kelvin wave $\lambda=2\pi/k$.[19] A previous grid measurement[14] found that Kelvin waves with a wavelength of 5 μm are excited on vortex lines attached to the grid mesh and that they create vortex rings at the threshold velocity. However, the grid amplitude at the onset of vortex generation is estimated to be ~ 0.1 μm, which is too small to cause the Kelvin waves to become unstable. In our case of smooth vibrating wires, the Kelvin waves are estimated to have a wavelength of $\lambda \sim 60$ μm from the frequency of the 47 Hz vibrating wire. This value is consistent with the amplitude of the wire motion at the onset of vortex generation, which is estimated to be $A=2v/\omega=74$ μm. This wire motion amplitude is sufficiently large to cause the Kelvin waves to become unstable. Also, the distance between the edges of a vortex line should be greater than half the wavelength of the Kelvin wave (30 μm), which is much greater than the wire thickness (3 μm). It is thus possible that the remanent vortices are attached not to the wire surfaces but to the wire and the walls of the silver box. In contrast, vortex generation by remanent vortices was not observed at any pressure for the 183 Hz vibrating wire. The wavelength of the Kelvin wave with a frequency of 183 Hz is estimated to be $\lambda \sim 30$ μm from Eq. (1). Therefore, the 183 Hz wire requires a velocity of about 20 mm/s to cause the Kelvin waves to become unstable at $A \sim \lambda$. Similar to the discussion regarding the vortex-avalanche model in the previous paragraph, vortex generation by remanent vortices could not be observed for the 183 Hz vibrating wire because pair breaking occurred below 20 mm/s. So far, we have only obtained one data point that reveals novel vortex-generation characteristics. Measurements using other low-frequency vibrating wires are necessary to confirm this measurement.

IV. CONCLUSIONS

We performed experiments using low-frequency vibrating wires by varying the pressure. For the 183 Hz vibrating wire at all pressures and the 47 Hz vibrating wire at 1 bar, vortex generation is observed at a velocity close to the velocity at which Cooper pairs break. This result indicates that vortices are generated by pair breaking. However, for the 47 Hz vibrating wire at 10, 20, and 28 bars, vortex generation is observed at a velocity lower than the pair-breaking velocity, independent of pressure. This result indicates that another vortex-generation mechanism may occur for the 47 Hz vibrating wire. This threshold velocity for vortex generation is found to be high enough to cause instability of the Kelvin wave for vortices attached to the wire, suggesting that vortices are generated by remanent vortices attached to the wire. It is necessary to perform experiments using vibrating wires with different frequencies to clarify this mechanism. However, it is difficult to perform such experiments in superfluid ^{3}He because of pair breaking. In superfluid ^{4}He, on the other hand, experiments over a wide range of frequencies have revealed that the critical velocity of the turbulent transition is proportional to the square root of the frequency.[19] Therefore, it is also necessary to study the generation of turbulence in superfluid ^{4}He, to clarify vortex generation due to instability of the Kelvin wave in superfluid ^{3}He.

ACKNOWLEDGMENTS

We would like to thank V. B. Eltsov, R. Hänninen, M. Krusius, and M. Tsubota for stimulating discussions. This research was supported by a Grant-in-Aid for JSPS (Grant No. 21-6355) and a Grant-in-Aid for Scientific Research on Priority Areas (Grant No. 17071008) from MEXT.

*ynago@sci.osaka-cu.ac.jp

[1] W. F. Vinen and R. J. Donnely, Phys. Today **60**(4), 43 (2007).
[2] P. C. Hendry, N. S. Lawson, P. V. E. McClintock, C. D. H. Williams, and R. M. Bowley, Phys. Rev. Lett. **60**, 604 (1988).
[3] O. Avenel and E. Varoquaux, Phys. Rev. Lett. **55**, 2704 (1985).
[4] R. J. Donnelly, *Quantised Vortices in Helium II* (Cambridge University Press, Cambridge, 1991).
[5] G. P. Bewley, D. P. Lathrop, and K. R. Sreenivasan, Nature (London) **441**, 588 (2006).
[6] D. D. Awschalom and K. W. Schwarz, Phys. Rev. Lett. **52**, 49 (1984).
[7] J. Jäger, B. Schuderer, and W. Schoepe, Phys. Rev. Lett. **74**, 566 (1995).
[8] H. Yano, N. Hashimoto, A. Handa, M. Nakagawa, K. Obara, O. Ishikawa, and T. Hata, Phys. Rev. B **75**, 012502 (2007).
[9] H. A. Nichol, L. Skrbek, P. C. Hendry, and P. V. E. McClintock, Phys. Rev. E **70**, 056307 (2004).
[10] M. Blažková, M. Človečko, V. B. Eltsov, E. Gažo, R. de Graaf, J. J. Hosio, M. Krusius, D. Schmoranzer, W. Schoepe, L. Skrbek, P. Skyba, R. E. Solntsev, and W. F. Vinen, J. Low Temp. Phys. **150**, 525 (2008).
[11] N. Hashimoto, R. Goto, H. Yano, K. Obara, O. Ishikawa, and T. Hata, Phys. Rev. B **76**, 020504(R) (2007).
[12] R. Hänninen, M. Tsubota, and W. F. Vinen, Phys. Rev. B **75**, 064502 (2007).
[13] S. N. Fisher, A. J. Hale, A. M. Guénault, and G. R. Pickett, Phys. Rev. Lett. **86**, 244 (2001).
[14] D. I. Bradley, D. O. Clubb, S. N. Fisher, A. M. Guénault, R. P. Haley, C. J. Matthews, G. R. Pickett, V. Tsepelin, and K. Zaki, Phys. Rev. Lett. **95**, 035302 (2005).
[15] J. P. Carney, A. M. Guénault, G. R. Pickett, and G. F. Spencer, Phys. Rev. Lett. **62**, 3042 (1989).
[16] A. P. Finne, V. B. Eltsov, G. Eska, R. Hänninen, J. Kopu, M. Krusius, E. V. Thuneberg, and M. Tsubota, Phys. Rev. Lett. **96**, 085301 (2006).
[17] Ü. Parts, V. M. H. Ruutu, J. H. Koivuniemi, Y. M. Bunkov, V. V. Dmitriev, M. Fogelström, M. Huebner, Y. Kondo, N. B. Kopnin, J. S. Korhonen, M. Krusius, O. V. Lounasmaa, P. I. Soininen, and G. E. Volovik, Europhys. Lett. **31**, 449 (1995); V. M. H. Ruutu, Ü. Parts, J. H. Koivuniemi, N. B. Kopnin, and M. Krusius, J. Low Temp. Phys. **107**, 93 (1997).
[18] D. I. Bradley, Phys. Rev. Lett. **84**, 1252 (2000); M. Niemetz, W. Schoepe, and M. Krusius, *ibid.* **87**, 059601 (2001); D. I. Bradley and G. R. Pickett, *ibid.* **87**, 059602 (2001).
[19] R. Hänninen and W. Schoepe, J. Low Temp. Phys. **153**, 189 (2008); arXiv:0801.2521 (unpublished).
[20] Y. Nago, M. Inui, R. Kado, K. Obara, H. Yano, O. Ishikawa, and T. Hata, J. Phys.: Conf. Ser. **150**, 032071 (2009).
[21] Y. Nago, T. Ogawa, A. Mori, Y. Miura, K. Obara, H. Yano, O. Ishikawa, and T. Hata, J. Low Temp. Phys. **158**, 443 (2010).
[22] H. Nakagawa, R. Kado, K. Obara, H. Yano, O. Ishikawa, T. Hata, H. Yokogawa, and M. Yokoyama, Phys. Rev. B **76**, 172504 (2007).
[23] M. P. Enrico, S. N. Fisher, and R. J. Watts-Tobin, J. Low Temp. Phys. **98**, 81 (1995), and references therein.
[24] C. A. M. Castelijns, K. F. Coates, A. M. Guénault, S. G. Mussett, and G. R. Pickett, Phys. Rev. Lett. **56**, 69 (1986).
[25] It is because a vortex-tangle region is expected to be limited to the most active region and the peak-to-peak amplitude of the wire; R. Goto, S. Fujiyama, H. Yano, Y. Nago, N. Hashimoto, K. Obara, O. Ishikawa, M. Tsubota, and T. Hata, Phys. Rev. Lett. **100**, 045301 (2008); H. Yano, Y. Nago, R. Goto, K. Obara, O. Ishikawa, and T. Hata, Phys. Rev. B **81**, 220507(R) (2010).
[26] V. M. H. Ruutu, V. B. Eltsov, A. J. Gill, T. W. B. Kibble, M. Krusius, Yu. G. Makhlin, B. Plaçais, G. E. Volovik, and W. Xu, Nature (London) **382**, 334 (1996).
[27] Below the velocity of 5 mm/s, resolutions of the frequency became worse because of low signal-to-noise ratios.
[28] H. Yano, T. Ogawa, A. Mori, Y. Miura, Y. Nago, K. Obara, O, Ishikawa, and T. Hata, J. Low Temp. Phys. **156**, 132 (2009).